Locating micro-seismic sources with a single seismometer channel using coda wave interferometry

LOCATING MICRO-SEISMIC SOURCES WITH A SINGLE SEISMOMETER CHANNEL USING CODA WAVE INTERFEROMETRY

(Right Running Head: Locate microseismic with a single sensor)

Youqian Zhao

Affiliation: School of GeoSciences, University of Edinburgh, Edinburgh, Midlothian, Scotland

E-mail address: s1159611@sms.ed.ac.uk

Andrew Curtis

Affiliation: School of GeoSciences, University of Edinburgh, Edinburgh, Midlothian, Scotland

E-mail address: Andrew.Curtis@ed.ac.uk

Brian Baptie

Affiliation: British Geological Survey, Edinburgh, Midlothian, Scotland

E-mail address: bbap@bgs.ac.uk

Original paper date of submission: 31-Jul-2016

Revised paper date of submission: 05-Oct-2016

ABSTRACT

A novel source location method based on coda wave interferometry (CWI) was applied to a micro-seismic dataset of mining induced events recorded in Nottinghamshire, England. CWI uses scattered waves in the coda of seismograms to estimate the differences between two seismic states. Here CWI is used to estimate the distances between pairs of earthquake locations, which are then used jointly to determine the relative location of a cluster of events using a probabilistic framework. We introduce two improvements to this location technique: these account for the impact of large difference in the dominant wavelength of recording made on different instruments, and standardize the selection of parameters to be used when implementing the method. While the method has been shown to produce reasonable estimates on larger earthquakes, we test the method for microseismic events with shorter distinguishable codas in recorded waveforms, and hence fewer recorded scattered waves. The earthquake location results are highly consistent when using different individual seismometer channels, showing that it is possible to locate event clusters with a single-channel seismometer. We thus extend the potential applications of this cost-effective method to seismic events over a wider range of magnitudes.

INTRODUCTION

Finding relative locations of seismic events is essential for discriminating earthquake fault and auxiliary planes from the sequences of aftershocks or foreshocks (Got et al., 1994), studying earthquake interaction and recurrence (Chen et al., 2012), and monitoring stress state and induced (micro)seismicity (Ellsworth, 2013). Instead of obtaining the relative locations of a cluster of events from their absolute locations which are typically subject to inaccuracies in subsurface velocity models, they are preferably estimated directly from travel-time differences between early arriving body waves, for example using joint hypocenter determination (Douglas, 1967; Dodge et al., 1995) or master event location (Deichmann and Garcia-Fernandez, 1992). The double-difference method of Waldhauser and Ellsworth (2000) locates clusters of earthquakes distributed over larger distances than the dominant recorded seismic wavelength when a dense seismic station network is available. However, in areas with fewer stations or unfavorable event-to-seismometer azimuthal coverage, the performance of the double-difference method deteriorates. In such circumstances, a recently developed source

location method based on coda wave interferometry (Snieder et al., 2006) would be particularly useful if proven to be reliable over the range of earthquake magnitudes of interest.

Coda refers to the later part of a seismogram, generated by multiply scattered waves. Seismic coda is disregarded in many seismological applications due to its complex appearance with few uniquely identifiable arrivals. However, the coda is extremely sensitive to small changes in the seismic system. Aki (1969) used the spectrum of coda from local earthquakes to estimate seismic moments, and more recently Snieder et al. (2002) developed coda wave interferometry (CWI) to use phase information to infer differences between pairs of sources or changes in the medium. CWI has been used to determine the relative velocity changes in the Earth's subsurface (Poupinet et al., 1984) and other solid materials, and to monitor changes in the interior of volcanoes (Wegler et al., 2006). A third range of application of CWI emerged is to estimate source separation between earthquakes with similar source mechanisms (Snieder and Vrijlandt, 2005; Robinson et al., 2011). The resulting source separations are used by Robinson et al. (2013) to determine the relative location of earthquakes, in which they demonstrate that CWI appears to outperform conventional location methods when the number of seismic stations is low.

CWI requires that the recorded coda contains waves that leave the source in many directions, and which are then multiply scattered towards the seismometers by heterogeneities in the medium. Robinson et al. (2013) tested the method on events with long codas; hence on data that contained many scattered arrivals per event. In our implementation of this novel technique, we apply the method to a micro-earthquake dataset from a colliery in Nottinghamshire, England, for which the codas are relatively short. We thus test the location technique in a new region, and for sources for which the theoretical requirements of CWI are less obviously fulfilled. Additionally, the magnitude range is such that the method might have significant common industrial as well as academic and hazard-related applications. We find that source separation estimates are highly consistent and the earthquake location results agree to within estimated uncertainties when using different individual seismometer channels. Therefore, it is possible to locate these earthquakes with a single-channel seismometer. We also discuss two issues that arise during the implementation and provide solutions as they may be encountered by other authors in the future.

DATA

The British Geological Survey (BGS) deployed a temporary seismic recoding network of 4 three-component (NOLA, NOLD, NOLE and NOLF) and 3 Z-component (NOLB, NOLC and NOLG) stations from February 2014, after some small earthquakes were detected in and around New Ollerton, Nottinghamshire since the middle of December 2013 (Figure 1a). This is a region where historical seismic activity is related to coal-mining. We selected 50 micro-earthquakes with the magnitudes 0.7-1.8 ML, with the criteria that 1) the signal-to-noise ratio is sufficiently high for the first arrivals to be identified, 2) recorded waveforms contain a distinguishable coda, and 3) the waveform of each event has a maximum correlation coefficient larger than some threshold with waveforms of at least four other events. Dominant frequencies among the different seismic station channels vary between ~2.5-10 Hz. All waveforms were filtered to 2-20 Hz before processing.

ESTIMAING SOURCE SEPARATION WITH CWI

Coda wave interferometry constrains the separation between a pair of sources by comparing the two seismogram codas recorded at each station. The theory is based on scattering path summation (Snieder, 1999) whereby the total wavefield at a given location is written as the superposition of waves traveling along all possible trajectories,

$$u^1(t) = \sum_T A_T(t)\,, \tag{1}$$

where u^1 is the total wavefield from event 1, T represents a wave trajectory, and A_T is the contribution to the total wavefield of waves that travel along trajectory T. All scattered wave trajectories can be divided into the path from the source to the first scatterer, and the path followed thereafter. If two nearby and similar sources are compared, CWI assumes that the paths to the first scatterers change, but that subsequent paths do not since they depend mainly on the medium rather than the source: the latter paths simply redistribute the small changes in energy arriving at the first scatterers over space and time throughout the coda. As a consequence, the dominant difference in recorded waveforms is in coda arrival times (Snieder, 2006). Equation 1 represents the waveform of one source recorded at an arbitrary station, so that of another closely-located source with identical mechanism recorded at the same station is $u^2(t) = \sum_T A_T(t - \tau_T)$, where τ_T is the travel-time difference of waves traveling along trajectory T due to the difference in source position. Since the two sources are located close together the two waveforms will be similar, which can be quantified by the normalized

cross-correlation of the two waveforms in a time-window defined with a central time t and a half-width t_ω, calculated for a sequence of time-windows in the coda

$$(t_s) = \frac{\int_{t-t_\omega}^{t+t_\omega} u^{(1)}(t')u^{(2)}(t'+t_s)dt'}{\sqrt{\int_{t-t_\omega}^{t+t_\omega} {u^{(1)}}^2(t')dt' \int_{t-t_\omega}^{t+t_\omega} {u^{(2)}}^2(t')dt'}} \quad (2).$$

In each time-window, the distribution of the travel-time differences τ_T contains information about the source separation δ (which can be in any direction). Snieder et al. (2006) estimates the standard deviation of the travel-time difference σ_τ from the maximum of the correlation coefficient R_{max}. σ_τ can then be related to the source separation δ by ${\sigma_\tau}^2 = \frac{1}{3}\frac{\delta^2}{v^2}$ for an isotropic source in an acoustic medium (where v is the velocity), or by ${\sigma_\tau}^2 = \frac{6/\alpha^8+7/\beta^8}{7(2/\alpha^6+3/\beta^6)}\delta^2$ (where α and β are P- and S-wave velocity) for a double-couple source in an elastic medium (Snieder and Vrijlandt, 2005). As the waves arriving in different time-windows have traveled along different paths, the separation results of each time-window are independent and are used to estimate uncertainty.

We conducted a series of synthetic experiments using multiply-scattered waveforms generated with the acoustic Foldy method (Foldy 1945; Galetti et al., 2013) in a $16 \times 16\ km^2$ medium with 150 random point scatterers within a velocity of 3000 m/s, with receivers throughout. Twenty sources are located around the center of the medium with Ricker wavelet time functions of equal length, with small inter-source distances compared to the dominant wavelength, ensuring similarity in their synthetic waveforms. The results show that individual inter-source separations computed from different coda time-windows from any one receiver fluctuated by up to 12.8% of their mean across all time windows, and that mean estimates for any one receiver lie within the uncertainty bounds of any other single receiver. Such results provide confidence, but do not include real-world effects such as true heterogeneity, double-couple sources or elastic effects, for which we turn to the real data.

As the theory of CWI requires identical source mechanisms, we classified the 50 New Ollerton micro-earthquakes into three groups with 33, 10 and 7 events respectively. Source similarity in each group is assured by waveform similarity, assessed by cross-correlation. For each group, we picked the first arrivals of waveforms recorded by the same channels of seismic stations and aligned them. We assume differences in coda are due only to varying source locations; this is not true if seismic velocity also changes. While the two types of

changes might be discriminated (Snieder et al. 2002), this is beyond our scope. Figure 1 shows the similarity of waveforms within one group, and compares early arrivals and coda of the same pair of waveforms.

We computed inter-source separations with data from each individual station. Coda windows begin at 26s, and assumed P- and S-wave velocities around the sources are 4088 m/s and 2298 m/s. Figure 2(a) shows the 21 inter-source separations from the 7 events in group 3. Each data point is the mean of results calculated for all available time-windows from each useable channel in each waveform pair, with the standard deviation of each mean displayed in panel (b). The results show that source separations and uncertainties are consistent between individual independent stations. Before passing the separation data to the location process, those pairs whose means were estimated to be smaller than their standard deviations were rejected.

SOURCE LOCATION

Our source location algorithm estimates relative location from the separation estimates and their uncertainties. It also accounts for a known bias – an increasing tendency towards underestimation of larger true source separations due to cycle-skipping in the correlation of coda in Equation 2. To quantify this bias, Robinson et al. (2011) apply a conditional probabilistic density function (pdf) $P(\tilde{\delta}_t|\tilde{\delta}_{CWI})$, the probability of the true separation being $\tilde{\delta}_t$ given that the estimate from CWI is $\tilde{\delta}_{CWI}$, where the tilde above the separations indicates that the quantities are normalised by the dominant wavelength λ_d in recorded data. The source separation estimates from CWI are always smaller than λ_d, so both $\tilde{\delta}_t$ and $\tilde{\delta}_{CWI}$ are smaller than 1. According to Bayes' theorem, the posterior probability of $\tilde{\delta}_t$ is proportional to the likelihood of observing $\tilde{\delta}_{CWI}$ given the true separation $\tilde{\delta}_t$ multiplied by the prior on $\tilde{\delta}_t$,

$$P(\tilde{\delta}_t|\tilde{\delta}_{CWI}) \propto P(\tilde{\delta}_{CWI}|\tilde{\delta}_t) \times P(\tilde{\delta}_t) \quad (3).$$

The prior is used to incorporate information about source separation or event location known prior to the location process, which here is considered to be a uniform distribution with wide bounds. The likelihood function $P(\tilde{\delta}_{CWI}|\tilde{\delta}_t)$ is approximated by a positively bounded Gaussian pdf by establishing empirical functions for its mean $\mu = \mu(\tilde{\delta}_t)$ and standard deviation $\sigma = \sigma(\tilde{\delta}_t)$ given a true separation $\tilde{\delta}_t$. These empirical functions are derived from a multitude of synthetic experiments with a large range of true separations in different Gaussian random media, by fitting the rational function forms

$$\mu(\tilde{\delta}_t) = a_1 \frac{a_2 \tilde{\delta}_t^{\,a_4} + a_3 \tilde{\delta}_t^{\,a_5}}{a_2 \tilde{\delta}_t^{\,a_4} + a_3 \tilde{\delta}_t^{\,a_5} + 1},$$

$$\sigma(\tilde{\delta}_t) = c + b_1 \frac{b_2 \tilde{\delta}_t^{\,b_4} + b_3 \tilde{\delta}_t^{\,b_5}}{b_2 \tilde{\delta}_t^{\,b_4} + b_3 \tilde{\delta}_t^{\,b_5} + 1}, \quad (4)$$

where a_1,…, a_5 are found to be 0.4661, 48.9697, 2.4693, 4.2467 and 1.1619, respectively; in $\sigma = \sigma(\tilde{\delta}_t)$, b_1,…, b_5, c are 0.1441, 101.0376, 120.3864, 2.8430, 6.0823 and 0.017, respectively, and location results do not change significantly with small changes in parameter values. Equation 3 holds for each earthquake pair, given the separation data from different time windows for each channel used. Robinson et al. (2013) incorporate the separations between multiple event pairs by multiplying the formulae for all available event pairs, assuming they are independent of each other

$$P(\boldsymbol{e}_1, \dots, \boldsymbol{e}_n | \tilde{\delta}_{CWI}) = c \prod_{i=1}^{n} P(\boldsymbol{e}_i) \times \prod_{i=1}^{n-1} \prod_{j=i+1}^{n} P(\tilde{\delta}_{CWI,ij} | \boldsymbol{e}_i, \boldsymbol{e}_j) \quad (5)$$

where c is a constant, n is the number of events, $\boldsymbol{e}_i = (x_i, y_i, z_i)$ is event i location, within the last term we use $\delta_{t,ij} = \|\boldsymbol{e}_i - \boldsymbol{e}_j\|_2$ for source separation $\delta_{t,ij}$ between the i'th and j'th earthquakes, and the prior $P(\boldsymbol{e}_i)$ only contains the relative event locations. The maximum of the joint posterior pdf occurs at the most probable combination of the events locations. Taking the negative logarithm of equation 5, the multiplication is converted to summations, and the optimization is solved as a minimization problem using a conjugate gradient method.

We made two improvements to this location method. First, in each iteration of the minimization process, current event locations are used to compute the inter-event separations δ_t, which are then normalized to give the value of the joint posterior. However, the dominant frequency; hence dominant wavelength of micro-earthquakes often extends over a large range, and is also subject to limitations of recording instruments. In this study, the dominant wavelength among different channels varies between 190m and 760m: using the average dominant wavelength over different channels/stations therefore introduces inaccuracy to the location process. To this end, when conducting multiple-channel location we apply an individual likelihood for each channel, so that the inter-event separations computed during the iterations are normalized by the actual wavelengths. Thus when data from m channels are used, Equation 5 is modified to

$$P(\boldsymbol{e}_1, \dots, \boldsymbol{e}_n | \tilde{\delta}_{CWI}) = c \prod_{i=1}^{n} P(\boldsymbol{e}_i) \times \prod_{k=1}^{m} \prod_{i=1}^{n-1} \prod_{j=i+1}^{n} P_k(\tilde{\delta}_{CWI,ij} | \boldsymbol{e}_i, \boldsymbol{e}_j) \quad (6)$$

where k is the index over m channels.

Second, when specifying the number and length of coda time-windows for CWI, we want separation estimates to be consistent among different windows. Using data from different station channels, we find that the most consistent set of windows varies. Instead of using a trial and error method to fix these two fundamental parameters, we conduct a systematic search for an optimal combination that results in the lowest uncertainty of separations calculated between all events using CWI.

We compute a separation-uncertainty matrix for each channel (e.g. Figure 3): for each combination of parameters the matrix element is $\Omega_{i,j} = \sum_N \sigma_{i,j}/N$, where $\sigma_{i,j} = \sqrt{\sum_l (\delta_{i,j,k} - \bar{\delta}_{i,j})^2/l}$ is the standard deviation of separation estimates from l coda time windows for events i and j, $\delta_{i,j,k}$ is the separation estimate of the kth window and $\bar{\delta}_{i,j}$ is their mean, and N is the number of event pairs on that channel. The value of $\Omega_{i,j}$ reflects the uncertainty of separation estimates derived from one recording channel for each source pair. Averaging over multiple source pairs gives a final uncertainty estimate for that combination of parameters (we require at least four estimates to calculate a reasonable standard deviation). Figure 3 shows a typical matrix for the New Ollerton earthquakes, indicating that using four 4-second windows will give the most consistent separation estimates. The values of Ω appear to increase with the number of windows when windows are longer than 4.5s but this is due to micro-seismic codas being short: with more than three such windows, newly added windows are no longer suitable for CWI. This systematic approach thus frees us from the vagaries of trial and error methods and from using undefined or subjective quality metrics, and allows CWI technique to be automated.

For each of the three groups, minimization of the negative logarithm of the joint location pdf is conducted 10 times with different randomly distributed initial location. Figure 4(a) shows the location of group 3 with all available data from 11 seismic station channels, averaged over the results of the 10 experiments, and the variability between the 10 is indicated by 95% confidence ellipses. The average coordinate variability is only 12.7m and the minimizations therefore seem likely to have converged to the same (global) minimum, given the uncertainties in the source separation data. We located the events using data from each channel individually, and find that the estimated locations follow roughly consistent patterns. Figure 4(b)-(d) shows the estimated locations using single-channel stations NOLC, NOLD and NOLF; each gives similar results to those obtained using all available data. The

other two groups exhibit similar levels of uncertainty. Some event pairs are more or less separated than their CWI estimates because the optimization attempts to satisfy all distances at once which is generally impossible due to separation uncertainties. Nevertheless, location results of single channels or stations all share similar average patterns, even though the stations lie on very different azimuths from the event cluster (see Figure 1a). This is achieved because the coda in each time-window contains waves leaving the source from many directions; thus diminishing the sensitivity of the location result to the source-receiver azimuth. For comparison, the double-difference (DD) method with damping parameter 40 or 100 using data from all channels, gives results similar to CWI (c.f. right panel of Figure 4a with 4e and 4f). Across all three groups, locations from the two methods give fairly similar patterns with comparable spatial spreads using damping 40 (Figure 4g), and the DD cluster shrinks with damping 100 (Figure 4h).

CONCLUSION

Our application of the CWI-based source location method to the New Ollerton earthquakes demonstrates that this method is applicable to micro-seismicity and to industrial as well as academic purposes. It also shows that the location results with individual stations are highly consistent, as long as recorded seismograms have a sufficient length of coda. This computationally inexpensive method therefore adds a new technique to the arsenal for seismological applications that require accurate locations of local earthquakes without dense seismometer arrays.

ACKNOWLEDGMENT

We thank British Geological Survey (BGS) for providing the seismic data of New Ollerton earthquakes. Youqian Zhao is grateful for funding provided by the School of GeoSciences, University of Edinburgh and BGS. We also thank Dr. Giovanni Meles for his help at early stage.

REFERENCES

Aki, K., 1969, Analysis of seismic coda of local earthquakes as scattered waves: Journal of Geophysical Research, **74**, 615-631.

Chen, K. H., R. Bürgmann, and R. M. M. Nadeau, 2013, Do earthquakes talk to each other: Triggering and interaction of repeating sequences at Parkfield: Journal of Geophysical Research Solid Earth, **118**, 165-182.

Deichmann, N., and M. Garciafernandez, 1992, Rupture geometry from high-precision relative hypocenter locations of microearthquake clusters: Geophysical Journal International, **110**, 501-517.

Dodge, D. A., G. C. Beroza, and W. L. Ellsworth, 1995, Foreshock sequence of the 1992 landers, California, earthquake and its implications for earthquake nucleation: Journal of Geophysical Research Solid Earth, **100**, 9865-9880.

Douglas, A., 1967, Joint epicenter determination: Nature, **215**, 47-48.

Ellsworth, W. L., 2013, Injection-induced earthquakes: Science, **341**, 1225942(1-7).

Foldy, L. L., 1945, The multiple scattering of waves. 1. General theory of isotropic scattering by randomly distributed scatterers: Physical Review, **67**, 107-119.

Galetti, E., D. Halliday, and A. Cutis, 2013, A simple and exact acoustic wavefield modeling code for data processing, imaging, and interferometry applications: Geophysics, **78**, F17-F27.

Got, J. L., J. Frechet, and F. W. Klein, 1994, Deep fault plane geometry inferred from multiplet relative relocation beneath the south flank of Kilauea: Journal of Geophysical Research Solid Earth, **99**, 15375-15386.

Poupinet, G., W. L. Ellsworth, and J. Frechet, 1984, Monitoring velocity variations in the crust using earthquake doublets: an application to the Calaveras Fault, California: Journal of Geophysical Research, **89**, 5719-5731.

Robinson, D. J., M. Sambridge, and R. Snieder, 2011, A probabilistic approach for estimating the separation between a pair of earthquakes directly from their coda waves: Journal of Geophysical Research, **116**,1-14.

Robinson, D. J., M. Sambridge, R. Snieder, and J. Hauser, 2013, Relocating a Cluster of Earthquakes Using a Single Seismic Station: Bulletin of the Seismological Society of America, **103**, 3057-3072.

Robinson, D. J., R. Snieder, and M. Sambridge, 2007, Using coda wave interferometry for estimating the variation in source mechanism between double couple events: Journal of Geophysical Research Solid Earth, **112**, B12302

Snieder, R., 1999, Imaging and averaging in complex media in diffuse waves in complex media: Springer Netherlands.

Snieder, R., 2006, The theory of coda wave interferometry: Pure and Applied Geophysics, **163**, 455-473.

Snieder, R., A. Gret, H. Douma, and J. Scales, 2002, Coda wave interferometry for estimating nonlinear behavior in seismic velocity: Science, **295**, 2253.

Snieder, R., and M. Vrijlandt, 2005, Constraining the source separation with coda wave interferometry: Theory and application to earthquake doublets in the Hayward fault, California: Journal of Geophysical Research Solid Earth, **110**, B04301.

Waldhauser, F., and W. L. Ellsworth, 2000, A double-difference earthquake location algorithm: Method and application to the northern Hayward fault, California: Bulletin of the Seismological Society of America, **90**, 1353-1368.

Wegler, U., B. G. Luhr, R. Snieder, and A. Ratdomopurbo, 2006, Increase of shear wave velocity before the 1998 eruption of Merapi volcano (Indonesia): Geophysical Research Letters, **33**, L09303

FIGURES

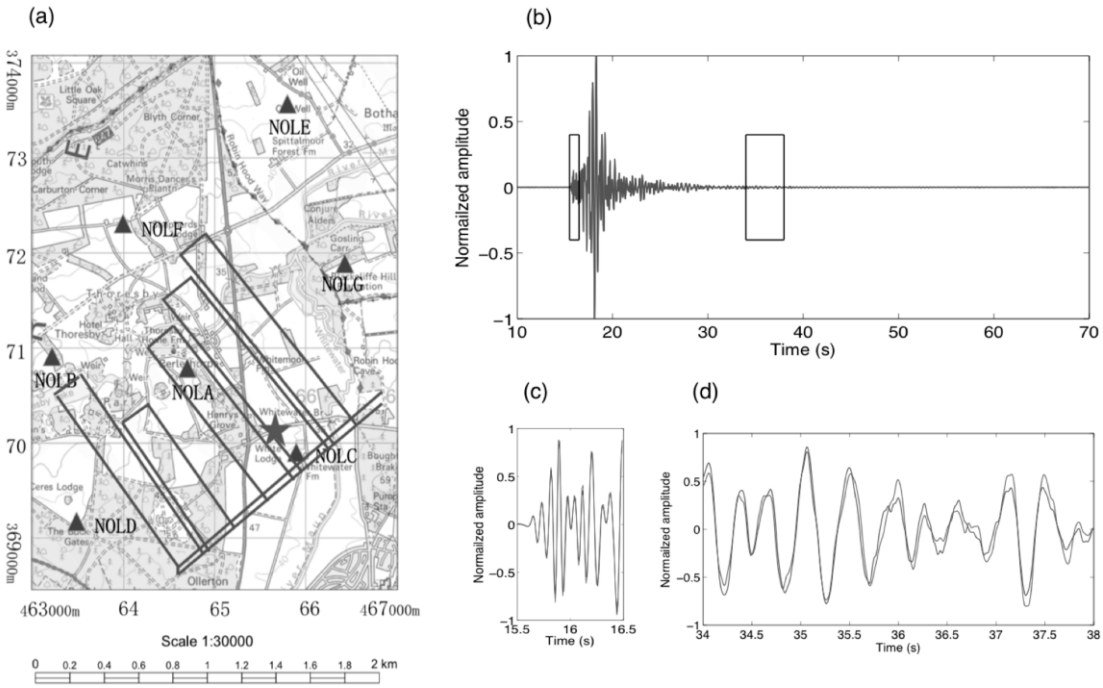

Figure 1: Map of the source region and typical waveforms. Panel (a) shows Thorsby colliery, New Ollerton, Nottinghamshire, England. The star shows the area around which the micro-earthquakes are likely to have occurred, triangles are temporary seismic stations, and the rectangles indicate locations of subsurface mining galleries. Panel (b)-(d) show the waveforms of two earthquakes in event Group 3 recorded by the N-channel of station NOLF, where (b) shows the whole waveforms, (c) and (d) show a 1-second window around the first arrival, and one of the time-windows (4 seconds) in the coda respectively, both indicated by boxes in (b). A comparison between panel (c) and (d) indicates that coda is more sensitive to source locations than early arrivals.

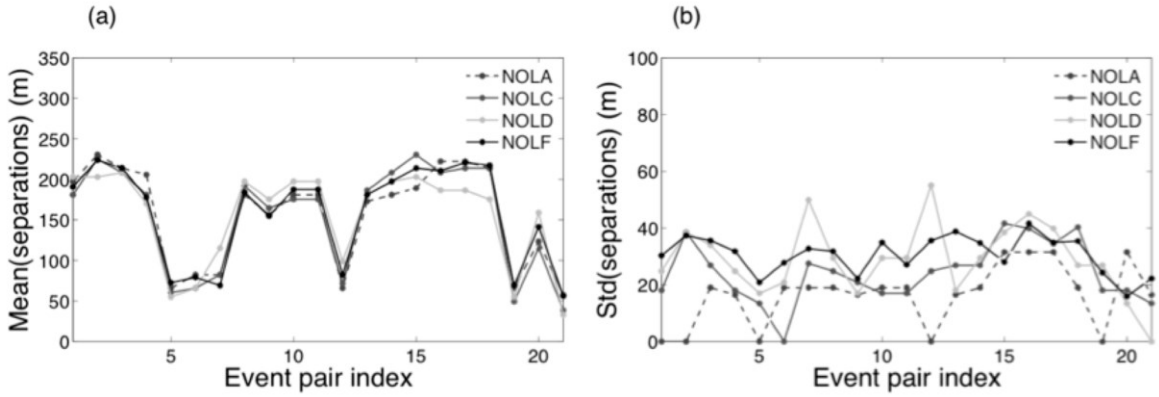

Figure 2: Source separations estimated with single station channels. Each point in panel (a) shows the mean of the five estimates; each corresponding point in panel (b) shows the standard deviation.

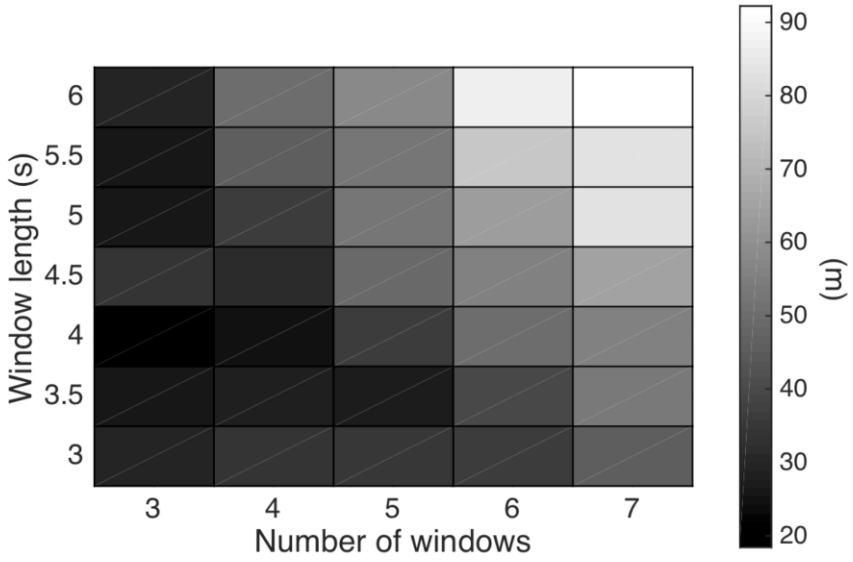

Figure 3: Separation-uncertainty matrix of the single-channel station NOLC. Colors indicate values of the average standard deviations resulting from the corresponding combination of number and length of time-windows used to divide coda. As a minimum of four time-windows are required for calculating standard deviations, the values for three windows are only shown here for illustration.

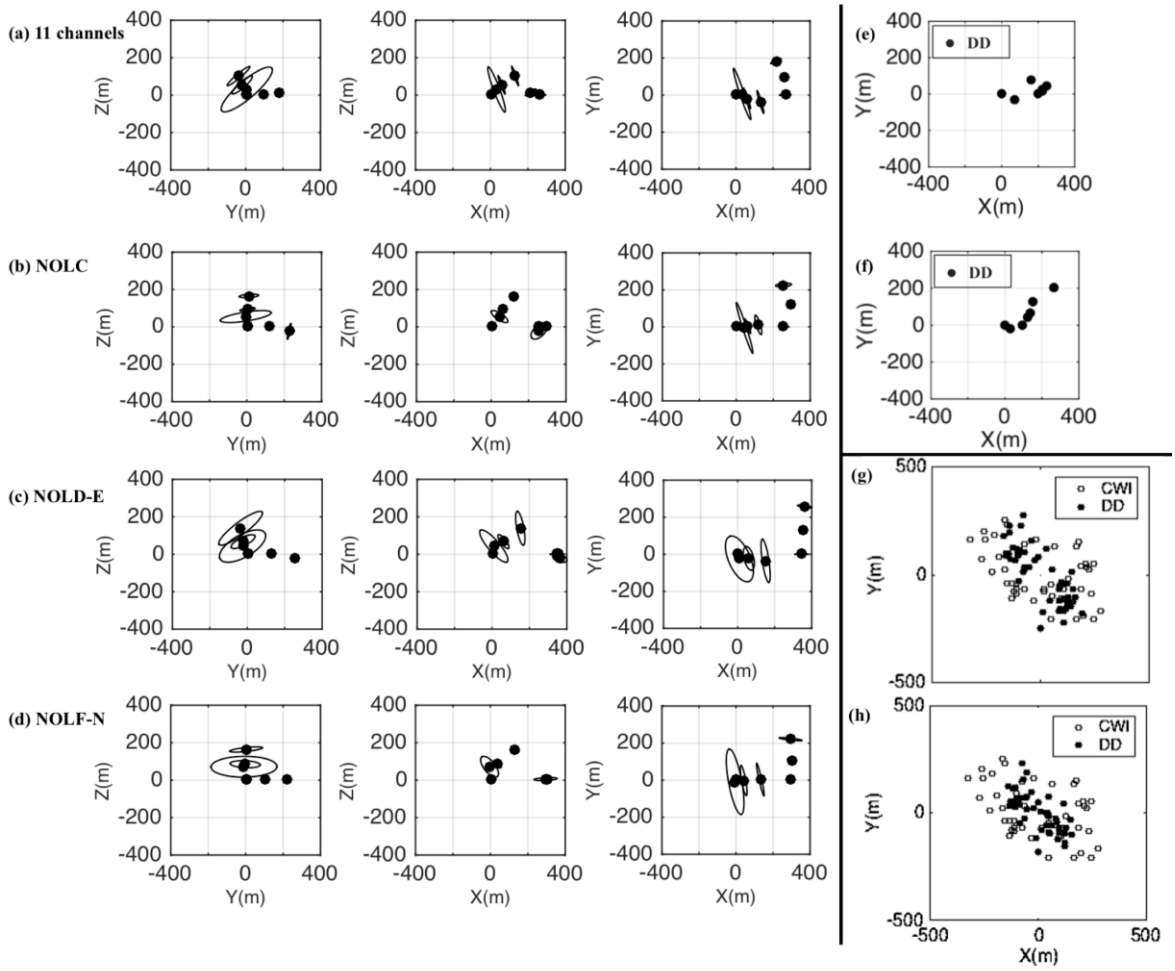

Figure 4: Planar projections of relative location results. Axes X, Y and Z point to three orthogonal directions. Panels (a-d) show the CWI results of group 3, where dots are the event mean locations averaged over 10 location optimizations; ellipses show 95% confidence intervals in the means. Panel (a) shows results obtained using all available data from 6 stations (11 channels). Panels (b) – (d) each shows the results from single channels from stations NOLC, NOLD and NOLF, respectively. Panels (e) and (f) show location results of the Double-Difference method with damping parameter 40 and 100, respectively. Panels (g) and (h) show comparisons of location results of CWI (hollow circles) and Double-Difference method (solid circles), with damping values in Double-Difference method of 40 and 100, respectively.